Single-Electron-Phonon Interaction in a Suspended Quantum Dot Phonon Cavity

E. M. Weig,[1,*] R. H. Blick,[1,†] T. Brandes,[2] J. Kirschbaum,[1] W. Wegscheider,[3] M. Bichler,[4] and J. P. Kotthaus[1]

[1]*Center for NanoScience & Sektion Physik, Ludwig-Maximilians-Universität, 80539 München, Germany*
[2]*Department of Physics, University of Manchester, Institute of Science and Technology (UMIST), Manchester M60 1QD, United Kingdom*
[3]*Institut für Angewandte und Experimentelle Physik, Universität Regensburg, 93040 Regensburg, Germany*
[4]*Walter-Schottky-Institut, Technische Universität München, 85748 Garching, Germany*

(Received 7 April 2003; published 30 January 2004)

An electron-phonon cavity consisting of a quantum dot embedded in a freestanding GaAs/AlGaAs membrane is characterized using Coulomb blockade measurements at low temperatures. We find a complete suppression of single electron tunneling around zero bias leading to the formation of an energy gap in the transport spectrum. The observed effect is induced by the excitation of a localized phonon mode confined in the cavity. This phonon blockade of transport is lifted at discrete magnetic fields where higher electronic states with nonzero angular momentum are brought into resonance with the phonon energy.

DOI: 10.1103/PhysRevLett.92.046804 PACS numbers: 73.23.Hk, 71.38.–k, 73.21.La, 73.63.Kv

In the context of quantum computation the operation of qubits is limited by the decoherence induced by the coupling to the environment [1]. One of the major sources of decoherence for solid state qubits based on single electron transistors (SETs) [2] and quantum dots [3] is the electron-phonon interaction. Its impact on single electron tunneling was initially explored by Fujisawa *et al.* [4] and Qin *et al.* [5] and theoretically confirmed by Brandes and Kramer [6]. Thus, the next step towards control of dephasing of electronic quantum states is to restrain coupling to the environment by confining the phonon spectrum in quantum dot cavities. Moreover, tailoring the mode spectrum of the phonon cavity opens up the possibility to investigate the ultimate limit of single electrons interacting with individual phonon modes of their host crystal. This is achieved by embedding a low-dimensional electron gas into a suspended phonon cavity [7–9].

Already back in 1967, Duke *et al.* [10] modeled inelastic tunneling through a barrier, finding that collective phonon modes can be excited by the tunneling electron. According to their calculations characteristic zero-bias conductance minima in the tunnel conductance can be attributed to this effect. In recent years, electron backaction on mechanical degrees of freedom has been theoretically discussed by Schwabe *et al.* [11], Blencowe [12], and Nishiguchi [13]. The additional implications of phonon confinement in an electron-phonon cavity were modeled by Debald *et al.* [14], pointing out the possibility to control electron dephasing by tailoring the phonon spectrum.

Here we report on the experimental observation of a new blocking mechanism of single electron transport which is found in such a cavity [cf. inset of Fig. 1(a) showing the differential conductance in the linear transport regime], evidencing the coherent interplay between single electron tunneling and the excitation of localized phonon modes confined in the cavity as predicted by Duke *et al.* [10]. The underlying physics of coherently coupling discrete electronic states with discrete phonon modes bears resemblance to cavity QED [15].

A phonon cavity containing a suspended single quantum dot is shown in Fig. 1(a). The scanning electron micrograph taken under an angle of 65° allows us to visualize the three-dimensional character of the sample. The freestanding 130 nm thick GaAs/AlGaAs membrane contains a low-dimensional electron gas which is located 40 nm below the sample surface. The 400 nm thick sacrificial layer of $Al_{0.8}Ga_{0.2}As$ supporting the membrane has been completely removed beneath the displayed part of the sample in Fig. 1(a) creating a clear spacing between the membrane and the GaAs buffer. Details on the employed sample material as well as the fabrication procedure can be found in previous publications [8,9]. The quantum dot is located in a 600 nm wide bar between two geometrically defined point contacts formed by pairs of symmetric indentations. As a result of edge depletion the dot diameter is reduced to about 450 nm [8]. The two constrictions are wide enough to allow ballistic transport through the cavity, but can be depleted to form tunneling barriers. In Fig. 1(a) a strip of electron gas situated close by serves as an in-plane gate electrode.

The presented measurements are performed in a dilution refrigerator with a base temperature of $T = 10$ mK which corresponds to a minimal electron temperature of $T_e = 100$ mK. A negative voltage V_g is applied to the gate electrode in order to create tunneling barriers and to vary the electrochemical potential of the dot denoted $\mu(N+1) = E(N+1) - E(N)$ in the level diagrams of Fig. 1(b) discussed below. A bias voltage V_{sd} can be applied between the source and the drain reservoirs. The differential conductance $G = dI_{sd}/dV_{sd}$ is recorded with respect to both V_g and V_{sd} showing clear Coulomb diamonds depicted in logarithmic gray scale representation in the left part of Fig. 2 (white: 0.02 μS, black:

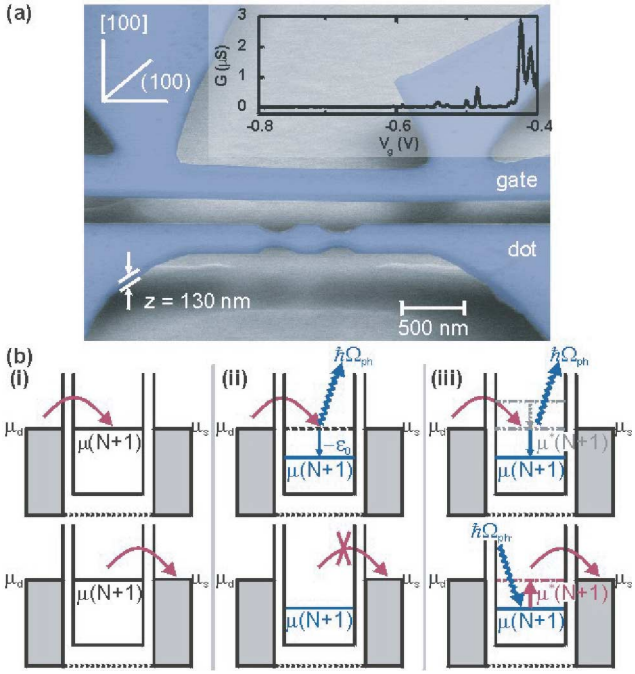

FIG. 1 (color online). (a) Suspended quantum dot cavity and in-plane gate formed in the 130 nm thin GaAs/AlGaAs membrane. The inset shows the blocked differential conductance in the linear transport regime. (b) Level diagrams for single electron tunneling including phonon blockade: (i) In the orthodox model electrons sequentially tunnel through the dot, if the chemical potential $\mu(N+1)$ is aligned between the reservoirs. (ii) Tunneling into the phonon cavity results in the excitation of a cavity phonon with energy $\hbar\Omega_{\mathrm{ph}}$, leading to a level mismatch ϵ_0 and thus to phonon blockade. (iii) Single electron tunneling is reestablished by a resonant higher electronic state $\mu^*(N+1)$ which is enabled to coherently reabsorb the phonon and to hereby replace the ground state.

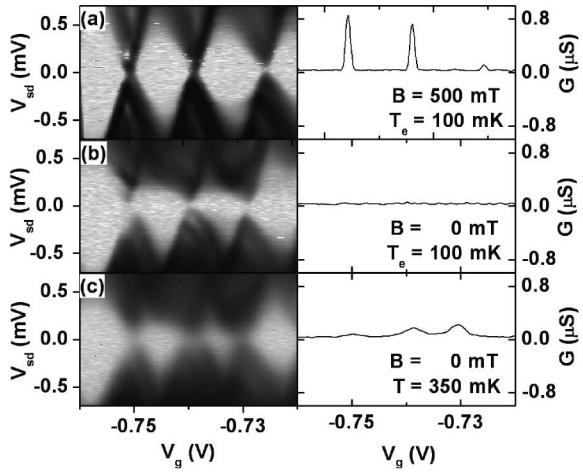

FIG. 2. Transport spectrum of the suspended quantum dot and conductance near zero bias: (a) Single electron resonances taken at an electron temperature of 100 mK and a perpendicular magnetic field of 500 mT. (b) At zero magnetic field conductance is suppressed for bias voltages below 100 μV due to phonon excitation. (c) The conductance pattern at 350 mK shows that phonon blockade starts to be surpassed because of thermal broadening of the Fermi function supplying empty states in the reservoirs.

6 μS). The right part of the figure displays the corresponding line plots near zero bias $V_{\mathrm{sd}} \approx 0$ μV. Figure 2(a) shows data taken at an electron temperature of $T_{\mathrm{e}} = 100$ mK and a perpendicular magnetic field of $B =$ 500 mT, where a quasicontinuum of energetically higher states produces a Coulomb blockade diamond known from conventional quantum dots [3,16]. The charging energy $E_{\mathrm{C}} = e^2/\mathrm{C}_\Sigma = 0.66$ meV corresponds to a dot capacitance of $C_\Sigma = 240$ aF from which a dot radius of $r = 275$ nm and an electron number of about 1400 can be deduced. The striking difference as compared to conventional quantum dot measurements is observed for the same temperature but zero magnetic field where we find complete suppression of conductance around zero bias for gate voltages $V_{\mathrm{g}} < -600$ mV [cf. inset of Fig. 1(a)]. As illustrated for the three adjacent resonances in Fig. 2(b), this is seen in the energy gap ϵ_0 opening between the diamonds in the gray scale plot as well as in the line plot showing zero conductance. The resulting blockade of transport can be overcome only by applying a positive or negative source drain bias of $|V_{\mathrm{sd}}| = \epsilon_0/e = 100$ μV [see also Fig. 3(a) magnifying a single resonance]. As discussed in [17] the curvilinear shape of the diamonds may reflect gate voltage induced mechanical deformations of the system. At larger temperatures the electrons gain enough energy to overcome phonon blockade when the broadening of the Fermi distribution function in the leads approaches $4k_{\mathrm{B}}T \approx \epsilon_0$. This is displayed in Fig. 2(c), where clear single electron tunneling resonances are found again at $T = 350$ mK and $B = 0$ T.

A strikingly similar energy gap has been observed in measurements on a single C_{60} SET [18]. Our results can therefore be compared to recent theoretical models for transport through such a molecular single electron transistor coupled to a single vibrational mode [19–21]. We have extended these models [22] in order to analyze the origin of the observed blockade mechanism. The picture corresponding to the classical limit of a strongly overdamped vibration mode is illustrated in Fig. 1(b): (i) In case of a conventional, nonsuspended SET sequential single electron tunneling occurs whenever Coulomb blockade can be overcome. This is the case if the electrochemical potentials of source, drain, and the dot μ_{s}, μ_{d}, and $\mu(N+1)$ are aligned such that the $(N+1)$th electron can tunnel elastically. This situation can be compared to the elastic emission of a gamma-ray photon from a nucleus embedded in a crystalline matrix described by the well-known Mössbauer effect [23]: The crystal takes up the recoil of the photon as a whole so that no recoil energy is transferred to the solid, and the photon energy remains constant. (ii) This behavior changes dramatically for a quantum dot embedded in a suspended phonon cavity [24]. Microscopic calculations of the phonon spectrum in a cavity orientated in the [100] direction perpendicular

to the sample surface reveal van Hove singularities in the cavity phonon density of states which are accompanied by an extreme enhancement of phonon emission [14]. As a result of this strong electron-phonon coupling, single electron tunneling induces mechanical excitation of the suspended quantum dot in the form of a localized cavity phonon of energy $\hbar\Omega_{\mathrm{ph}}$. With a simple infinite thin-plate model the lowest van Hove singularity for a cavity thickness of $z = 130$ nm is found at $\hbar\Omega_{\mathrm{ph}} \approx 3\hbar c_{\mathrm{L}}/z = 73\ \mu$eV for quantized dilatational phonon modes ($\hbar\Omega_{\mathrm{ph}} \approx 145\ \mu$eV for flexural modes) with $c_{\mathrm{L}} = 4.77 \times 10^5$ cm/s being the longitudinal velocity of sound in bulk GaAs. This prediction compares well to the observed energy gap $\epsilon_0 = 100\ \mu$eV so that we conclude that quantized phonon modes are excited within the cavity. Other known mechanisms for suppression of conductance such as spin blockade or interference effects in single or double quantum dots are excluded by a detailed comparison of our findings with data from previous studies on bulk quantum dot systems [25].

Flensberg has shown [21] that in the strongly overdamped, classical limit (quality factor $Q = \Omega_{\mathrm{ph}}/\gamma \ll 1$ for small phonon lifetime γ^{-1}), the energy cost of the mechanical excitation goes along with a drop of the chemical potential $\mu(N+1)$ in the dot, which leads to a blockade of single electron tunneling. The energy gap $\epsilon_0 = g\hbar\Omega_{\mathrm{ph}}$ then depends on the Franck-Condon coupling constant g. For $Q \to 0$ the "Mössbauer picture" [10] applies in analogy to a single nucleus emitting a photon. Opposite to the situation described in part (i) of Fig. 1(b) the cavity now picks up the "recoil" energy of the tunneling electron whereas the electron system immediately relaxes to a new ground state. As a result the $(N+1)$ electron system remains in the phonon blockade at a reduced energy as depicted in part (ii) of Fig. 1(b). On the other hand, $Q \to \infty$ would correspond to coherent cavity phonons where the Franck-Condon factors yield a series of phonon sidebands $n\Omega$ with weights given by the Poisson distribution $e^{-g}g^n/n!$ at zero temperature with $n = 0$ corresponding to elastic tunneling.

To reestablish single electron tunneling, the energy transferred to the cavity can be regained as displayed in part (iii) of Fig. 1(b) where the cavity phonon is reabsorbed exciting a higher lying electronic state $\mu^*(N+1)$. To this end, the excited cavity phonon mode coherently exchanges energy with the provided electronic excited states $\mu^*(N+1)$ which can be understood in terms of (damped) Rabi oscillations [22].

The phonon gap ϵ_0 is recorded with a higher resolution in Fig. 3(a) showing the central region of Fig. 2(a) in the same gray scale. The conventional shape of the Coulomb diamonds is marked by solid lines. Clearly, the asymmetric shape of the gap can be discerned: The crossing of the two solid lines indicates the position of the missing single electron tunneling conductance peak. The onset of conductance [denoted $*$ in Fig. 3(a)] occurs at a slightly different value of V_{g} by which the half diamonds are

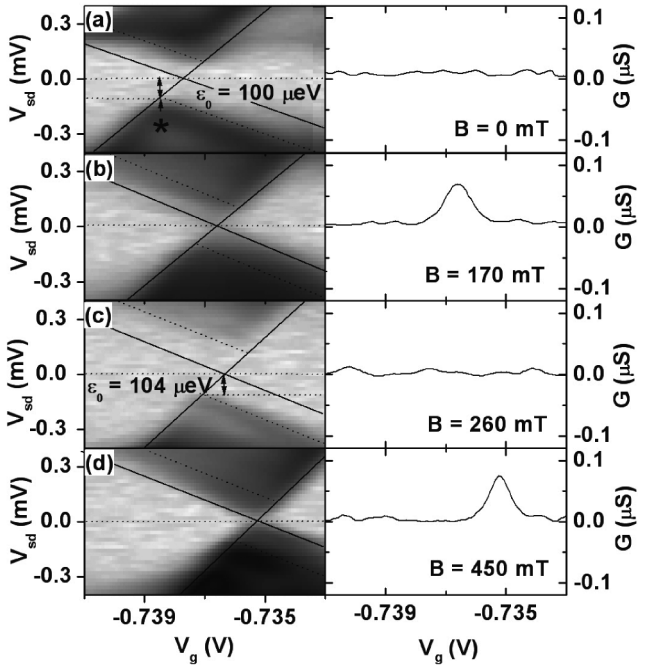

FIG. 3. Transport spectrum for (a) $B = 0$, (b) 170, (c) 260, and (d) 450 mT. The line plots give the conductance near zero bias. At certain magnetic fields (b),(d) excited quantum dot states with higher magnetic momentum are brought into resonance with the cavity phonon reenabling single electron tunneling. Otherwise (a),(c) transport is suppressed due to phonon blockade with an excitation barrier of around 100 μeV.

offset as indicated by dotted lines. This offset is also explained by the model developed in Fig. 1(b): At the onset of conductance at $V_{\mathrm{sd}} = \epsilon_0/e$ the energy level $\mu(N+1)$ must be aligned with the upper reservoir in order to permit single electron tunneling. Hence, the initial level position is shifted by $\delta V_{\mathrm{g}} = \epsilon_0/2e\alpha$ (where $\alpha = C_{\mathrm{g}}/C_{\Sigma}$) on the gate voltage axis.

In Figs. 3(b)–3(d) the same region is plotted for perpendicular magnetic fields of 170, 260, and 450 mT. It can be seen that for (b) and (d) phonon blockade is lifted leading to single electron tunneling resonances near zero bias. However, for the intermediate field in (c) the blockade is present. As mentioned above the lifting of the phonon blockade at low temperatures requires coherent coupling to an energetically higher lying state $\mu^*(N+1)$. According to the data displayed in Fig. 3 the excitation energies $\mu^*(N+1, B) - \mu(N+1, B=0)$ can be tuned in and off resonance [cf. part (iii) of Fig. 1(b)] by means of an applied magnetic field. We therefore conclude that the excited states $\mu^*(N+1)$ possess angular momentum $\ell\hbar$ ($\ell = 1, 2, \ldots$).

A direct comparison of the magnetic field dependence to transport spectroscopy on the dot is depicted in Fig. 4 where we consider two adjacent resonance peaks α (right, cf. Fig. 3) and β (left). In Fig. 4(a) conductance traces are recorded for bias voltages from 0 to $-800\ \mu$V at $B = 0$ mT with excited states marked lines. The zero-bias conductance is plotted logarithmically as a function of

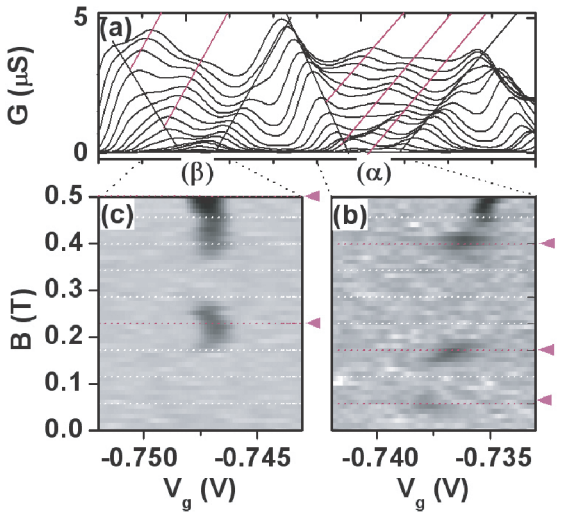

FIG. 4 (color online). (a) Line plot of conductance resonances α and β at different source drain bias voltages between 0 and -800 μV. Ground and excited states are marked by lines. The conductance at $V_{sd} \approx 0$ μV is suppressed. (b) Conductance near zero bias for resonance α plotted against gate voltage V_g and magnetic field B. Finite conductance appears for 57, 170, and 400 mT. (c) Similar plot for resonance β. Nonzero conductance is found for 230 and 510 mT.

both gate voltage V_g and magnetic field B for α and β in Fig. 4(b) (white: 0.01 μS, black: 0.2 μS) and 4(c) (white: 0.01 μS, black: 2 μS), respectively. For resonances α and β we find excited states at energies $\mu_\alpha^{*1} = 230$ μeV, $\mu_\alpha^{*2} = 440$ μeV, $\mu_\alpha^{*3} = 740$ μeV and $\mu_\beta^{*1} = 380$ μeV and $\mu_\beta^{*2} = 760$ μeV. Strikingly the number of states matches the number of discrete magnetic fields at which phonon blockade is lifted at 57, 170, and 400 mT in α and 230 and 510 mT in β. For higher magnetic fields the increasingly complex excitation spectrum [16] being characterized by multiple level crossings and mixing of states provides a quasicontinuum of excited states to fully restore single electron tunneling.

The presented measurements demonstrate that for freely suspended quantum dot cavities conductance near zero bias is completely suppressed as single electron tunneling gives rise to the excitation of a discrete cavity phonon. The resulting energy loss leads to a suppression of linear electron transport and to the formation of a distinct energy gap. This phonon blockade effect can be overcome at bias voltages large enough to bridge the energy gap, or at a sufficiently high bath temperature. A third mechanism circumventing phonon blockade is given by aligning higher lying electronic states such that electronic transport is enabled through these states after reabsorption of the cavity phonon in a process similar to Rabi oscillations.

We thank Stefan Debald for stimulating discussions. Support from the Bundesministerium für Forschung und Technologie and the Deutsche Forschungsgemeinschaft is acknowledged. R. H. B. thanks the EOARD for support.

*Electronic address: eva.weig@physik.uni-muenchen.de. Previous work has been published under the name of E. M. Höhberger.
†Present address: Electrical and Computer Engineering, University of Wisconsin–Madison, Madison, WI 53706, USA.

[1] D. V. Averin, Nature (London) **398**, 748 (1999); C. H. Bennett and D. P. DiVincenzo, Nature (London) **404**, 247 (2000).
[2] T. A. Fulton and G. J. Dolan, Phys. Rev. Lett. **59**, 109 (1987); H. Grabert and M. H. Devoret, *Single Charge Tunneling* (Plenum, New York, 1992).
[3] R. Ashoori, Nature (London) **379**, 413 (1996); L. P. Kouwenhoven *et al.*, *Mesoscopic Electron Transport* (Kluwer Academic, Dordrecht, 1997), pp. 105–214.
[4] T. Fujisawa *et al.*, Science **282**, 932 (1998).
[5] H. Qin *et al.*, Phys. Rev. B **64**, 241302(R) (2001).
[6] T. Brandes and B. Kramer, Phys. Rev. Lett. **83**, 3021 (1999).
[7] R. H. Blick *et al.*, Phys. Rev. B **62**, 17 103 (2000).
[8] J. Kirschbaum *et al.*, Appl. Phys. Lett. **81**, 280 (2002).
[9] E. M. Höhberger, T. Krämer, W. Wegscheider, and R. H. Blick, Appl. Phys. Lett. **82**, 4160 (2003).
[10] C. B. Duke, S. D. Silverstein, and A. J. Bennett, Phys. Rev. Lett. **19**, 315 (1967).
[11] N. F. Schwabe *et al.*, Phys. Rev. B **52**, 12 911 (1995).
[12] M. P. Blencowe, Physica (Amsterdam) **263B–264B**, 459 (1999).
[13] N. Nishiguchi, Phys. Rev. B **68**, 121305(R) (2003).
[14] S. Debald, T. Brandes, and B. Kramer, Phys. Rev. B **66**, 041301(R) (2002).
[15] A. Imamoglu *et al.*, Phys. Rev. Lett. **83**, 4204 (1999).
[16] P. A. Maksym, Physica (Amsterdam) **249B–251B**, 233 (1998); L. P. Kouwenhoven, D. G. Austing, and S. Tarucha, Rep. Prog. Phys. **64**, 701 (2001).
[17] S. Sapmaz, Ya. M. Blanter, L. Gurevich, and H. S. J. van der Zant, Phys. Rev. B **67**, 235414 (2003). Another possible cause for distorted Coulomb diamonds is discussed by S. J. Tans *et al.*, Nature (London) **394**, 761 (1998).
[18] H. Park *et al.*, Nature (London) **407**, 57 (2000).
[19] D. Boese and H. Schoeller, Europhys. Lett. **54**, 668 (2001).
[20] J.-X. Zhu and A. V. Balatsky, cond-mat/0210003.
[21] K. Flensberg, cond-mat/0302193; S. Braig and K. Flensberg, cond-mat/0303236.
[22] T. Brandes *et al.* (to be published).
[23] R. L. Mössbauer, Rev. Mod. Phys. **36**, 362 (1964).
[24] In a simplified classical picture the situation described in (i) is equivalent to the reflection of a particle at a hard wall of infinite mass, whereas the situations in (ii) and (iii) can be compared to a particle inelastically or elastically hitting a trampoline.
[25] A. K. Hüttel *et al.*, Europhys. Lett. **62**, 712 (2003); T. Heinzel *et al.*, Europhys. Lett. **26**, 689 (1994); A. W. Holleitner *et al.*, Science **297**, 70 (2002).